



LAWRENCE
LIVERMORE
NATIONAL
LABORATORY

Compact proton spectrometers for measurements of shock

A. Mackinnon, A. Zylstra, J. A. Frenje, F. H. Seguin, M. J. Rosenberg, H. G. Rinderknecht, M. Gatu Johnson, D. T. Casey, N. Sinenian, M. Manuel, C. J. Waugh, H. W. Sio, C. K. Li, R. D. Petrasso, S. Friedrich, K. Knittel, R. Bionta, M. McKernan, D. Callahan, G. Collins, E. Dewald, T. Doeppner, M. J. Edwards, S. H. Glenzer, D. Hicks, O. L. Landen, R. London, N. B. Meezan

May 7, 2012

19th Topical Conference High-Temperature Plasma
Diagnostics
Monterey, CA, United States
May 6, 2012 through May 10, 2012

Disclaimer

This document was prepared as an account of work sponsored by an agency of the United States government. Neither the United States government nor Lawrence Livermore National Security, LLC, nor any of their employees makes any warranty, expressed or implied, or assumes any legal liability or responsibility for the accuracy, completeness, or usefulness of any information, apparatus, product, or process disclosed, or represents that its use would not infringe privately owned rights. Reference herein to any specific commercial product, process, or service by trade name, trademark, manufacturer, or otherwise does not necessarily constitute or imply its endorsement, recommendation, or favoring by the United States government or Lawrence Livermore National Security, LLC. The views and opinions of authors expressed herein do not necessarily state or reflect those of the United States government or Lawrence Livermore National Security, LLC, and shall not be used for advertising or product endorsement purposes.

Compact proton spectrometers for measurements of shock ρR and shock strength in NIF implosions.

A. B. Zylstra,^{1, a)} J. A. Frenje,¹ F. H. Séguin,¹ M. J. Rosenberg,¹ H. G. Rinderknecht,¹ M. Gatu Johnson,¹ D. T. Casey,¹ N. Sinenian,¹ M. J.-E. Manuel,¹ C. J. Waugh,¹ H. W. Sio,¹ C.K. Li,¹ R.D. Petrasso,¹ S. Friedrich,² K. Knittel,² R. Bionta,² M. McKernan,² D. Callahan,² G. W. Collins,² E. Dewald,² T. Döppner,² M.J. Edwards,² S. Glenzer,² D. G. Hicks,² O. L. Landen,² R. London,² A. Mackinnon,² N. Meezan,² R. Prasad,² J. Ralph,² M. Richardson,² J. R. Rygg,² S. Sepke,² S. Weber,² R. Zacharias,² E. Moses,² ...,² J. Kilkenny,³ A. Nikroo,³ T. C. Sangster,⁴ V. Glebov,⁴ C. Stoeckl,⁴ ...,⁴ R. Olson,⁵ R. J. Leeper,⁵ J. Kline,⁶ G. Kyrala,⁶ and D. Wilson⁶

¹⁾ *Plasma Science and Fusion Center, Massachusetts Institute of Technology, Cambridge, MA, 02139 USA*

²⁾ *Lawrence Livermore National Laboratory, Livermore, CA 94550 USA*

³⁾ *General Atomics, San Diego, CA, 92186 USA*

⁴⁾ *Laboratory for Laser Energetics, University of Rochester, Rochester, NY 14623, USA*

⁵⁾ *Sandia National Laboratory, Albuquerque, NM 87185, USA*

⁶⁾ *Los Alamos National Laboratory, Los Alamos, NM, 87545 USA*

(Dated: 2 May 2012)

The compact Wedge Range Filter (WRF) proton spectrometer was developed for OMEGA and transferred to the National Ignition Facility (NIF) as a National Ignition Campaign (NIC) diagnostic. The WRF measures the spectrum of protons from D-³He reactions in tuning-campaign implosions containing D and ³He gas; in this work we report on the first proton spectroscopy measurement on the NIF using WRFs. The energy downshift of the 14.7-MeV proton is directly related to the total ρR through the plasma stopping power. Additionally, the shock proton yield is measured, which is a metric of the final merged shock strength.

PACS numbers: 52.70.Nc

I. INTRODUCTION

The National Ignition Facility (NIF) is a 1.8MJ 192 beam ignition-scale laser for Inertial Confinement Fusion (ICF) experiments¹. ICF requires proper assembly of the fusion fuel for ignition and burn^{2,3}. In particular, the cold DT (deuterium and tritium) fuel must reach a high enough areal density (ρR), which is primarily measured by the Magnetic Recoil Spectrometer (MRS)⁴⁻⁷ and neutron Time of Flight (nTOF) spectrometers⁸.

Non-cryogenic experiments are conducted as part of the NIF tuning campaign^{9,10}, such as Symmetry Capsule (SymCap) implosions¹¹ to tune the shape¹² and Convergent Ablation (ConvAbl) implosions¹³ to measure the velocity and remaining mass. In these capsules the cryogenic fuel layer is replaced with a surrogate mass of CH and the capsules are filled with a D₂ + ³He gas fuel mixture, which produces the fusion reaction $D + {}^3\text{He} \rightarrow {}^4\text{He}(3.6 \text{ MeV}) + p(14.7 \text{ MeV})$ among others.

Of particular interest is the 14.7 MeV proton from D³He fusion. By measuring the proton spectrum, the energy lost while traversing the implosion is known, and thus the line-integrated mass and total ρR are determined. This technique has been used extensively on the OMEGA laser facility¹⁴ to study implosion physics^{15,16}. Several Wedge Range Filter (WRF) spectrometers¹⁷ have been implemented at the OMEGA and NIF.

In ICF a series of shocks are driven into the capsule by a specifically shaped laser pulse. The shock timing is tuned so that the subsequent shocks catch up to the first, coalesce, then collapse in the core before the peak compression of the capsule. This gives two distinct nuclear production times, hereafter referred to as ‘shock’ and ‘compression’¹⁶⁻¹⁸.

Measurements of proton spectra during the Sym-Cap and ConvAbl campaigns give important observables

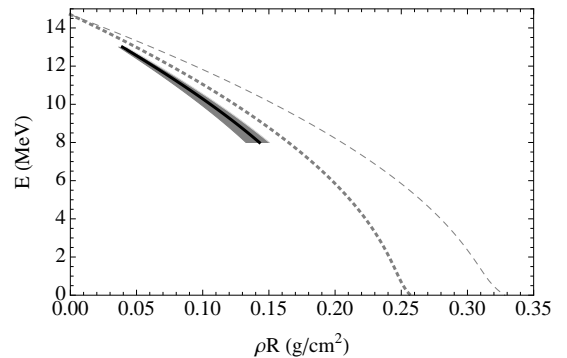


FIG. 1. D³He proton energy versus total ρR , calculated using the Li-Petrasso dE/dx for various ρR models: in a CH plasma with $T_e = T_i = 0.5 \text{ keV}$, $\rho = 100 \text{ g/cm}^3$ which represents the compression phase (dashed gray) and $\rho = 10 \text{ g/cm}^3$ for the shock phase (dotted gray). The black curve represents a HYDRA-derived model composed of fuel, shell, and ablated mass near shock burn with 50% error bars in ρ and T_e represented by the gray shaded region.

^{a)} Electronic mail: zylstra@mit.edu

which are used to study the effects of implosion tuning; for example this data sheds light on the in-flight mass profile and final merged shock strength, which impacts the hot-spot adiabat and shell deceleration. Additionally, these data could be systematically compared to radiation-hydrodynamics simulations in LASNEX¹⁹ and HYDRA²⁰ as a benchmark of those codes.

II. STOPPING POWER CALCULATIONS

To infer ρR from the energy loss we must calculate the stopping power for an energetic proton in a plasma. We use the Li-Petrasso stopping power model²¹ throughout this work. The simplest model assumes that all ρR comes from a spherical shell of CH plasma. At shock (compression) burn the convergence is low (high) and the shell is best represented by $\rho = 10(100)$ g/cm³. The measured proton energy versus implosion ρR is calculated using this model and shown in Fig. 1.

In reality, the in-flight ρR is composed of the nuclear fuel, remaining ablator material, and ablated mass. The fuel and ablated mass have much higher T_e and lower ρ than the cold shell, and therefore lower stopping power²¹. This is particularly important during the shock phase, when the remaining shell can have only $\sim 50\%$ of the total ρR , resulting in lower ρR for a given downshift compared to the spherical shell model (Fig. 1). Using a radiation-hydrodynamics simulation from HYDRA, we construct a model where mass-averaged ρ and T_e are taken for each of the three regions (fuel, shell, ablated mass) from the simulation. The shell convergence is then artificially varied to generate a curve of downshifted proton energy versus ρR .

We assume that this stopping model accurately reflects capsule conditions within $\pm 50\%$ in ρ and T_e (shaded region, Fig. 1). This error is added in quadrature with the precision of the WRF to give an absolute error in ρR .

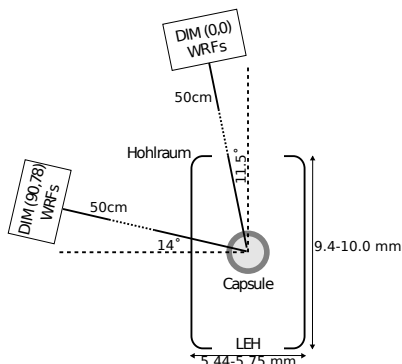


FIG. 2. Schematic of the experimental setup at NIF. The hohlraum is shown with capsule inside. The DIM (0,0) WRFs view the implosion through the Laser Entrance Hole (LEH) at an angle of 11.5° to the hohlraum axis, while the DIM (90,78) WRFs view through the hohlraum wall at an angle of 14° to the equator.

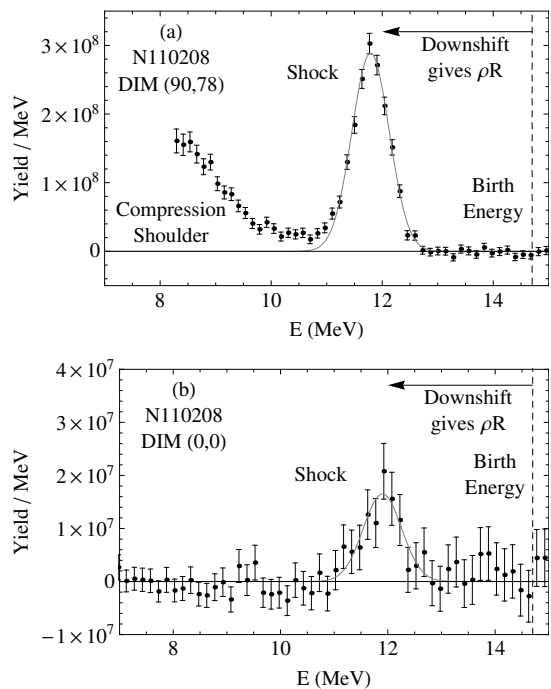


FIG. 3. D^3He proton spectrum measured on NIF shot N110208 (1.3MJ SymCap shot with a 544 Au hohlraum) on DIM (90,78) (a), and DIM (0,0) (b). The downshift from the birth energy at 14.7 MeV (dashed line) gives the ρR . Gaussian fits to the shock peak are shown in gray. On the equator, $Y_p = (2.43 \pm 0.44) \times 10^8$ and $E = 11.79 \pm 0.14$ MeV, corrected for the hohlraum downshift, corresponding to $\rho R = 68 \pm 8$ mg/cm². Between 8 – 10 MeV we see additional proton production associated with the start of compression burn; these protons are downshifted more than the shock protons meaning they were produced later in time at higher ρR . On the pole, we measured a yield of $Y_p = (1.48 \pm 0.35) \times 10^7$ and $E = 11.90 \pm 0.26$ MeV corresponding to $\rho R = 65 \pm 10$ mg/cm². Strong EM fields at the LEH deflect protons, resulting in the dramatic yield reduction compared to the equatorial data.

III. EXPERIMENTAL SETUP

Fig. 2 shows the NIF experimental setup. WRFs are fielded on Diagnostic Instrument Manipulators (DIMs), in particular on DIMs (0,0) and (90,78)²². One to two WRFs are fielded on each DIM²³. On DIM (0,0) the WRFs have a clear line of sight to TCC. The DIM (90,78) WRFs look through the hohlraum. Depending on the experimental campaign the hohlraum wall at this line of sight is up to $64\mu\text{m}$ of Au or DU and up to $74\mu\text{m}$ of Al²⁴. For some hohlraums one line of sight from DIM (90,78) is obscured by the thick Al thermo-mechanical band; this data is not used. All proton spectra are corrected for the hohlraum-induced energy downshift using cold-matter stopping powers²⁵, which is a valid approximation according to integrated hydrodynamics calculations.

The SymCap/ConvAbl capsule fill is generally 30:70 atomic D:³He. The total laser energy used was between

1MJ and 1.6MJ, with varying pulse shapes due to ongoing ignition tuning. The hohlraum material was Au or DU; the hohlraum geometry was varied between 5.44mm ('544') and 5.75mm ('575') outer diameter.

IV. DATA

Fig. 3 shows proton spectra measured on NIF Sym-Cap shot N110208, a 544 Au hohlraum, shot with 1.3MJ total laser energy. The areal density measured on the pole ($\rho R = 65 \pm 10$ mg/cm²) and equator ($\rho R = 68 \pm 8$ mg/cm²) are equivalent within error bars. Therefore this data is consistent with a symmetric in-flight implosion during the shock burn. However, simulations indicate $\rho R = 77 - 85$ mg/cm² at shock flash, suggesting that the implosion is at a larger radius (lower convergence) during the shock burn than predicted. This is also apparent as a difference in energy downshift, making it unlikely that the discrepancy can be explained by systematic ρR model uncertainties.

The shock proton yield measured on the equator [$Y_p = (2.43 \pm 0.44) \times 10^8$] is much higher than the polar measurement [$Y_p = (1.48 \pm 0.35) \times 10^7$]. This is due to strong transverse magnetic or electric fields at the LEH which deflect protons measured at DIM (0,0) but do not affect equatorial measurements (see Fig. 2). This is consistent with previous experiments²⁶⁻²⁸ at OMEGA. Using the equatorial measurement only, we compare to post-shot simulations that have $Y_p = 2.9 \times 10^9$ for this implosion, giving a yield over clean (YOC) of $\approx 10\%$.

V. CONCLUSIONS

We report the first proton spectra measured on the NIF in D:³He gas-filled indirect-drive implosions using the compact WRF spectrometer. The spectral shape is used to infer the shock proton yield, a measure of shock strength, and the in-flight ρR at shock flash time. Compared to hydrodynamics simulations, the shock proton yield is lower than modeled by a factor of 10 and the in-flight ρR at shock flash is lower, implying less shell convergence by shock flash. The WRFs have recorded high-quality data on over sixty NIF shots, including more than forty-five indirect-drive D:³He gas-filled implosions.

Extensive future work is planned for the large WRF data set at NIF: implementing the particle Time of Flight (pTOF) diagnostic²⁹ to measure the shock bang time, developing an implosion model describing the complete proton spectrum, using a Guderley self-similar imploding shock solution^{18,30} to infer the final merged shock strength from the proton yield, studying the observed field-induced proton deficits through the LEH, and using occasional observed asymmetries between the WRF lines of sight will be systematically studied to infer the implosion shape, particularly for P_2 modes.

ACKNOWLEDGMENTS

The authors thank the engineering, operations, and technical staff at NIF, LLE, and MIT for their sup-

port. This work was done in part for ABZ's Ph.D. thesis and was supported in part by the U.S. DoE (DE-FG52-09NA29553), LLNL (B580243), LLE (414090-G), the Fusion Science Center at the University of Rochester (415023-G), and the National Laser Users Facility (DE-NA0000877). This work was performed under the auspices of the U.S. Department of Energy by Lawrence Livermore National Laboratory under Contract DE-AC52-07NA27344. ABZ is supported by the DoE NNSA Stewardship Science Graduate Fellowship (DE-FC52-08NA28752).

- ¹G. Miller, E. Moses, and C. Wuest, *Nuclear Fusion* **44**, S228 (2004).
- ²J. Nuckolls, L. Wood, A. Thiessen, and G. Zimmerman, *Nature* **239**, 139 (1972).
- ³J. Lindl, *Physics of Plasmas* **2**, 3933 (1995).
- ⁴J. Frenje *et al.*, *Review of Scientific Instruments* **72**, 854 (2001).
- ⁵J. Frenje *et al.*, *Review of Scientific Instruments* **79**, 10E502 (2008).
- ⁶J. Frenje *et al.*, *Physics of Plasmas* **17**, 056311 (2010).
- ⁷D.T. Casey, *Diagnosing Inertial Confinement Fusion Implosions at OMEGA and the NIF Using Novel Neutron Spectrometry* (Massachusetts Institute of Technology, 2012).
- ⁸V. Glebov *et al.*, *Review of Scientific Instruments* **77**, 10E715 (2006).
- ⁹O. Landen *et al.*, *Physics of Plasmas* **17**, 056301 (2010).
- ¹⁰S. Glenzer *et al.*, *Science* **327**, 1228 (2010).
- ¹¹G. Kyrala *et al.*, *Physics of Plasmas* **18**, 056307 (2011).
- ¹²G. Kyrala *et al.*, *Review of Scientific Instruments* **81**, 10E316 (2010).
- ¹³D. Hicks, B. Spears, D. Braun, R. Olson, C. Sorce, P. Celliers, G. Collins, and O. Landen, *Physics of Plasmas* **17**, 102703 (2010).
- ¹⁴T. Boehly *et al.*, *Optics Communications* **133**, 495 (1997).
- ¹⁵R. Petrasso *et al.*, *Physical Review Letters* **90**, 95002 (2003).
- ¹⁶J. Frenje *et al.*, *Physics of Plasmas* **11**, 2798 (2004).
- ¹⁷F. Séguin *et al.*, *Review of Scientific Instruments* **74**, 975 (2003).
- ¹⁸J. R. Rygg, *Shock Convergence and Mix Dynamics in Inertial Confinement Fusion* (Massachusetts Institute of Technology, 2006).
- ¹⁹G. Zimmerman and W. Kruer, *Controlled Fusion* **2**, 51 (1975).
- ²⁰M. Marinak, G. Kerbel, N. Gentile, O. Jones, D. Munro, S. Pol-laine, T. Dittrich, and S. Haan, *Physics of Plasmas* **8**, 2275 (2001).
- ²¹C. Li and R. Petrasso, *Physical Review Letters* **70**, 3059 (1993).
- ²²The NIF DIMs are named by chamber coordinates (θ, ϕ) , where $\theta = 0$ is vertically up.
- ²³A new capability to field WRFs on DIM (90,78), mirrored below the equator from the present detectors, for a maximum of 4 detectors, is not discussed in this work.
- ²⁴The uncertainty in material thickness is ± 1 μm Au/DU and ± 3 μm Al. In some designs the Au/DU thickness changes by several μm over the detector solid angle. This primarily causes artificial line broadening but does not affect the mean energy.
- ²⁵J. Ziegler, J. Biersack, and U. Littmark, *The stopping and range of ions in matter* (Pergamon, New York, 1985).
- ²⁶C. Li *et al.*, *Physical Review Letters* **102**, 205001 (2009).
- ²⁷C. Li *et al.*, *Science* **327**, 1231 (2010).
- ²⁸F. Philippe *et al.*, *Physical Review Letters* **104**, 35004 (2010).
- ²⁹H. Rinderknecht *et al.*, Submitted to *Review of Scientific Instruments* (2012).
- ³⁰G. Guderley, *Luftfahrtforsch* **19**, 302 (1942).